International Journal of Enhanced Research in Science Technology & Engineering, ISSN: 2319-7463
Vol. 3 Issue 1, January-2014, pp: (383-388), Impact Factor: 1.252, Available online at: www.erpublications.com

Analytical Speedup for the Optimal Design of MEMS Touch Mode Capacitive Pressure Sensors

Joseph Riad[1], Mourad El-Gamal[2], Hani Ragai[1]
[1]Electronics and Communications Engineering Department, Ain Shams University, Cairo, Egypt
[2]Department of Electrical and Computer Engineering, McGill University, Montréal, Canada

Abstract: Obtaining an optimal design for micro electro-mechanical systems (MEMS) structures is a computationally-intensive and time-consuming task as it usually involves numerous non-linear finite-element method (FEM) simulations. This work presents an analytical method to achieve a near-optimal design for circular diaphragm touch mode capacitive pressure sensors and thus find an optimal design without relying on multiple FEM iterations. The resulting design is optimal in the sense of attaining maximum sensitivity for a given sensor radius or minimum radius for a given target sensitivity. The method presented here depends on a lower bound on sensor area derived from an analytical model. We show that this method can achieve significant improvement in terms of area or sensitivity compared to conventional designs.

Keywords: design , micro electro-mechanical systems, pressure sensors, touch mode

Introduction

Capacitive pressure sensors rely on the deflection of a movable diaphragm under the action of pressure. When the deflection changes due to a change in pressure, the sensor capacitance varies and this variation is used to measure the change in pressure. Such sensors have two principal modes of operation: normal mode, where the diaphragms don't come into contact and touch mode, where the diaphragms come into contact with a thin layer of dielectric in between. Fig. 1 shows the structure of a capacitive pressure sensor with a circular diaphragm and its two operating modes. Of the two modes, touch mode is preferred due to its higher sensitivity, better linearity and large pressure over-load protection[1-3].

The main challenge in the design of touch mode capacitive pressure sensors (TMCPS) lies in the difficulty to accurately model the sensor's deflection as the underlying mechanical contact problem has no exact, closed form solution [4, 5]. This intractability means that the design of TMCPS relies on non-linear finite-element method (FEM) simulations. Obtaining an optimized TMCPS design via FEM simulations is a computationally-intensive and time- consuming task. An optimized design is crucial, however, for systems where sensor area is quite limited such as pressure sensors operating in a harsh environment. Harsh environment applications usually rely on silicon carbide (SiC) transistors for interface electronics; such transistors are usually very large in size due to their inherently low mobility [6-8], which tends to make the sensor area very limited. A design with minimum sensor area, therefore, makes such systems feasible.

The analytical design flow proposed here makes use of existing approximate models from the literature [2,5,9] and a lower bound on total sensor area derived from the models.

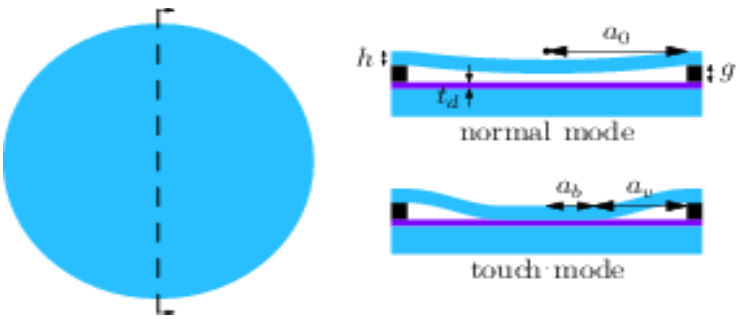

Figure 1. Circular diaphragm capacitive pressure sensor structure

Analytical Model

Fig. 1 defines the sensor parameters that will be used in the equations: h is the diaphragm thickness, g is the gap height at zero diaphragm deflection, a_0 is the diaphragm radius and t_d is the dielectric layer thickness. To obtain an approximate analytical model for the sensor characteristics, we make use of the well established virtual radius approach [2, 5] whereby the diaphragm radius is divided into two radii: the touching radius (a_b) and the non-touching radius (a_v) as shown in Fig. 1. The non-touching radius a_v at a specific pressure P is calculated by finding the radius of a virtual membrane whose center would just be touching the dielectric layer at P. The center point displacement w_0 at pressure P for a diaphragm of radius a is given by [9]:

$$w_0(P) = \frac{Pa^4}{64D}\left[\frac{1}{1+2\alpha\left(\frac{w_0}{h}\right)^2+\frac{\sigma_i h a^2}{16D}}\right] \qquad (1)$$

where D is the diaphragm's flexural rigidity, given by $D = \frac{Eh^3}{12(1-\nu^2)}$ where E is the diaphragm material's Young's modulus and ν is its Poisson's ratio. The factor α, a function only of ν, accounts for non-linear elastic behavior and has been calculated in [2]. The factor σ_i represents the diaphragm's residual stress due to fabrication. We can thus find the virtual radius (a_v):

$$a_v = \sqrt{\frac{2\sigma_i g h}{P}\left(1+\sqrt{1+\frac{16PD}{\sigma_i^2 h^2 g}\left[1+2\alpha\left(\frac{g}{h}\right)^2\right]}\right)} \qquad (2)$$

and the diaphragm's deflection profile in touch mode:

$$w(r,P) = \begin{cases} g, & 0 < r < a_b(P) \\ g\left[1-\left(\frac{r-a_b(P)}{a_v(P)}\right)^2\right]^2, & a_b(P) < r < a_0 \end{cases} \qquad (3)$$

Given the deflection profile, we can thus calculate the capacitance by dividing the gap into infinitesimal parallel plate capacitors. Following this approach, we find the total capacitance in touch mode to be [5]

$$C = C_d\left\{[1+2(k_1-k_2)(1-\gamma)]\frac{a_v^2}{a_0^2}+2[k_2(1-\gamma)-1]\frac{a_v}{a_0}+1\right\} \qquad (4)$$

where

$$C_d = \frac{\pi\varepsilon_0\varepsilon_d a_0^2}{t_d} \qquad \gamma = \frac{1}{\frac{t_d}{g\varepsilon_d}+1} \qquad k_1 = \frac{1}{2}\frac{\tanh^{-1}(\sqrt{\gamma})}{\sqrt{\gamma}}$$

$$k_2 = \frac{\tan^{-1}\left[\sqrt{\gamma}/\sqrt{\sqrt{\gamma}-\gamma}\right]}{2\sqrt{\sqrt{\gamma}-\gamma}} + \frac{\tanh^{-1}\left[\sqrt{\gamma}/\sqrt{\sqrt{\gamma}+\gamma}\right]}{2\sqrt{\sqrt{\gamma}+\gamma}}$$

and ε_d is the dielectric layer's relative permittivity.

Lower Bound on Area

Given the bounds of a required operating pressure range (P_1 and P_2), sensitivity is reported as the slope of the linear least squares fit to the sensor's $C-P$ characteristics [9]. For a first iteration, we'll ignore the terms α and σ_i in (2) and obtain an approximate expression for a_v:

$$a_v(P) = \sqrt[4]{\frac{64Dg}{P}} \qquad (5)$$

If we define the touch point pressure (P_T) as the pressure at which the membrane's center just touches the dielectric, we can write $a_v(P_T) = a_0$ and use this relation in conjunction with (4) and (5) to rewrite the sensor's capacitance as

$$C(P) = a\sqrt{\frac{P_T}{P}} + b\sqrt[4]{\frac{P_T}{P}} + c \qquad (6)$$

where

$$a = C_d[1+2(k_1-k_2)(1-\gamma)]$$
$$b = 2C_d[k_2(1-\gamma)-1]$$
$$c = C_d$$

Let the linear least squares fit have the form $\bar{C}(P) = a_1 P + a_2$.

By definition, a_1 and a_2 should be chosen to minimize the integral of squared deviation:

$$I(a_1, a_2) = \int_{P_1}^{P_2} \left[a\sqrt{\frac{P_T}{P}} + b\sqrt[4]{\frac{P_T}{P}} + c - a_1 P - a_2 \right] dP \qquad (7)$$

We thus require that

$$\frac{\partial I}{\partial a_1} = \frac{\partial I}{\partial a_2} = 0$$

These conditions translate into a system of linear equations that can be solved for a_1 and a_2. Equating the calculated a1 to the target sensitivity (S) results in a necessary condition for P_T:

$$\lambda(C_d)\sqrt{P_T} + \mu(C_d)\sqrt[4]{P_T} - S = 0 \qquad (8)$$

where

$$\lambda = \frac{[1+2(k_1-k_2)(1-\gamma)]}{\Delta} P_1^{\frac{5}{2}} (\beta - 1)\left(\frac{\beta^{\frac{3}{2}}-1}{3} - \beta + \sqrt{\beta} \right) \qquad (9a)$$

$$\mu = \frac{\{2[k_2(1-\gamma)-1]\}}{\Delta} P_1^{\frac{11}{4}} (\beta - 1)\left[\frac{2}{21}\left(\beta^{\frac{7}{4}} - 1\right) - \frac{2}{3}\left(\beta - \beta^{\frac{3}{4}}\right) \right] \qquad (9b)$$

$$\Delta = -\frac{[P_1(\beta-1)]^4}{12} \qquad (9c)$$

$$\beta \triangleq \frac{P_2}{P_1} > 1 \qquad (9d)$$

and we solve (8) to obtain

$$P_T = \left[-\frac{\mu}{2\lambda}\left(1 \pm \sqrt{1 + \frac{4S\lambda}{(C_d)\mu^2}} \right) \right]^4 \qquad (10)$$

We now proceed to show that $\lambda < 0$. First we note from (9c) that $\Delta < 0$ and

$$[1 + 2(k_1 - k_2)(1 - \gamma)] > 0 \quad \forall \gamma > 0$$

Finally, we note that

$$(\beta - 1)\left(\frac{\beta^{\frac{3}{2}} - 1}{3} - \beta + \sqrt{\beta} \right) > 0 \quad \forall \beta > 1$$

We have thus proven that $\lambda < 0$ independent of sensor dimensions and operating pressure range. This means that the square root term in (10) can be imaginary, which would lead to an unfeasible design. From this consideration, we reach a lower bound on area:

$$\pi a_0^2 \geq \frac{4t_d S(-\lambda)}{\varepsilon_0 \varepsilon_d \mu^2} \qquad a_0 \geq \widehat{a_0} = \sqrt{\frac{4t_d S(-\lambda)}{\pi \varepsilon_0 \varepsilon_d \mu^2}} \qquad (11)$$

A more accurate expression for the lower bound can be derived by taking α and σ_i into consideration. This is further explained in the appendix in order to keep the focus on the design flow.

Proposed Design Flow

Based on the discussion in the previous section, we propose the following design flows for obtaining a near-optimal design.

A. Minimum Area Design:

1. The dielectric thickness is set to the minimum value allowed by the fabrication technology. As can be seen from (11), the lower t_d , the lower the required sensor area.

2. The gap height g is set to a suitable value by selecting a value for γ. Fig. 2 plots the γ-dependent factor of $\widehat{a_0^2}$ given by

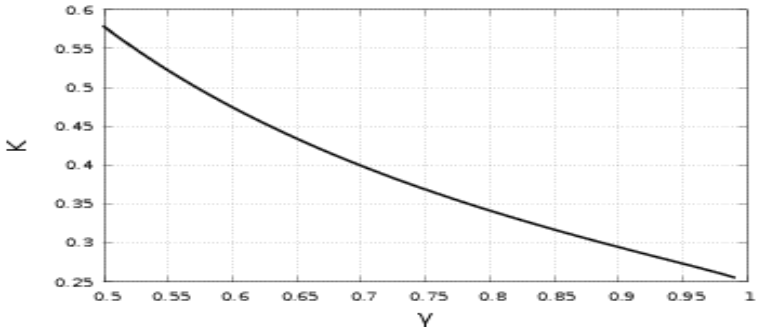

Figure 2. Choosing a value for g to maximize sensitivity per unit area.

$$K = \frac{1 + 2(k_1 - k_2)(1 - \gamma)}{4[k_2(1 - \gamma) - 1]^2}$$

As can be seen, the higher g (the higher γ), the better. The choice of how high γ can go depends on t_d and ε_d.

3. Using the given sensitivity and operating pressure range, $\widehat{a_0}$ found from (11).
4. Using (8), the required value for P_T (and hence h) is found.
5. The initial estimate for h is iteratively refined by using the more accurate expressions in (12) and (13).

B. Maximum Sensitivity Design:

1. The dielectric thickness is set to the minimum value allowed by the fabrication technology.
2. The gap height g is set to a suitable value by selecting a value for γ.
3. Using the given sensor area and operating pressure range, S is found from (11).
4. Steps 4-5 from the minimum area design flow are followed.

Results and Discussion

In order to validate the above analysis, the sensor designed in [9] is used as reference. The procedure used in [9] to design the sensor begins by selecting P_T such that the operating pressure range is within $1.2 - 2.5\ P_T$. For fixed g, h and t_d, one can thus find a_0 and the sensor design is complete. Using the same operating pressure range, we applied the design flows outlined in the previous section to obtain the minimum area for the same sensitivity and the maximum sensitivity for the same area. In both cases, γ was fixed at 0.97 in order to have the same g as the reported sensor design for a more valid comparison. Table 1 compares both designs to the published results. It is seen that following the proposed design flows can lead to a 25% reduction in area for the same sensitivity or a 30% increase in sensitivity for the same area.

To further validate the results, FEM simulation was carried out for both designs using COMSOL. To reduce the computational complexity of the model, the symmetry of the structure is exploited and a 2-dimensional axi-symmetric model is used. To further exploit the regularity of the structure, a mapped mesh is used to solve the model. Fig. 3 shows a schematic of the model structure along with the boundary conditions and load applied. The pressure load is ramped and the mechanical problem of finding the diaphragm's deflection is solved. To ensure that the diaphragm doesn't penetrate the lower electrode, a contact pair is defined between the two electrodes. Solving for the diaphragm deflection in the contact regime is what makes the problem highly non-linear and computationally expensive. Sensor capacitance is obtained via post-processing by integrating over the lower edge of the diaphragm. Fig. 4 shows the sensor characteristics for both designs. It can be seen that the models agree well in the normal operation mode but diverge in the touch mode. This is to be expected since the virtual radius approach is only approximate. A more accurate model of sensor characteristics may be obtained by similar considerations to the seventh

TABLE I. Comparison of published results and design results. g= 1.5 µm, t_d=350 nm and ε_d=7.5 (Si_3N_4)

	Published work [9]	Designed Sensors	
		Minimum Area	*Maximum Sensitivity*
a_0 (µm)	97	85	97
S (fF/kPa)	0.23	0.23	0.3
h (µm)	3	1.9	2.1

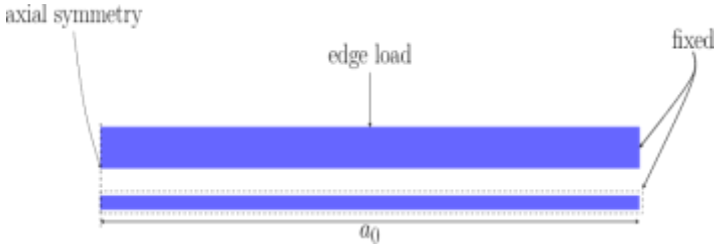

Figure 3. Schematic representation of the COMSOL model used

case in the seminal work by Timoshenko [10], which derives the characteristics of a uniformly-loaded circular membrane with a concentric circular hole. This approach was rejected here, however, because it does not lead to a closed form model and therefore does not lend itself to analytical methods.

Fig. 5 shows the sensor sensitivity as a function of *h* for both designs. It can be seen clearly that sensitivity is a concave function of *h* which means that the estimate for *h* can be further refined by running a simple single-variable convex optimization algorithm. Since the analytical model produced a value for h that is quite close to the optimum value, the optimizer can find the optimum in only a few iterations. This was carried out and the final values of *h* are reported in table 1. To demonstrate the speedup made possible by the analytical method, non-linear constrained optimization was performed for the values of a_0 , *g* and *h* with the values used by the work in [9] as an initial estimate and a non-linear constraint fixing the value of P_T to that chosen by [9]. Making use of MATLAB's optimization toolbox, multi-variable non-linear optimization was carried out (with a_0 , *g* and *h* as parameters). The results of the full optimization were compared to the results from the nonlinear single variable optimization (with only h as parameter). The comparison is reported in table 2. Note that only relative times are reported in order to make the results independent of the particular hardware and software used. The table shows a speedup of nearly 5 times made possible by the analytical method.

Conclusion

An analytical method for achieving a near-optimal design for circular diaphragm TMCPS was presented based on a lower bound on sensor radius. The analysis made use of the approximate virtual radius approach and quickly made accessible a near-optimal design in terms of sensitivity or area. It was further demonstrated that the analysis reduces the design space to a single parameter (*h*), which means that the design can be improved using a simple, single variable convex optimization algorithm instead of the computationally expensive multivariate optimization algorithm that would have been necessary with a multi-parameter design space. Comparing optimization methods in both cases showed that optimization based on the analytical method provided a 5 times speedup compared to optimization without analysis. Moreover, the reduction in area that can be achieved with this method enables the use of sensors in applications where the sensor area is severely limited such as harsh environment applications.

TABLE II. Comparison between single-variable optimization made possible by analysis and multi-variable optimization required otherwise.

	MATLAB Optimization Algorithm	Iterations	Objective Function Evaluations	Relative Time
Proposed Method	fminbnd	5	5	1X
Without Analysis	fmincon	5	24	4.9X

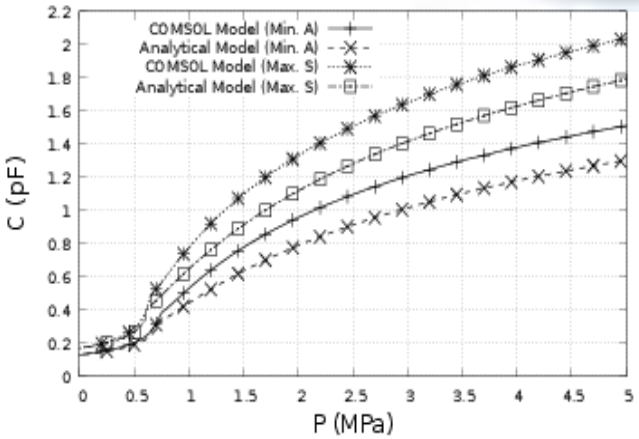

Figure 4. Characteristics of the designed sensors

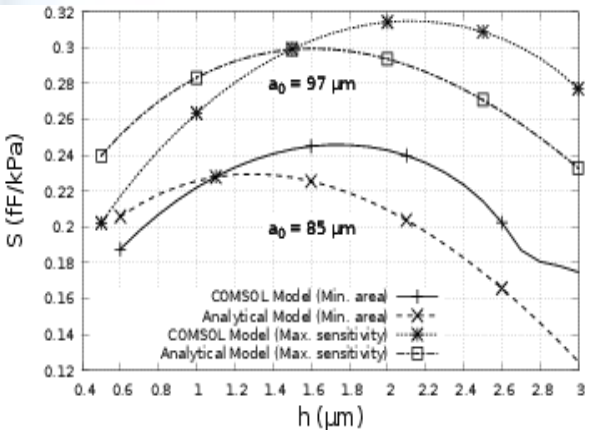

Figure 5. Sensitivity vs. *h* for the designed sensors.

References

[1]. W. H. Ko and Q. Wang, "Touch mode capacitive pressure sensors," Sensors and Actuators A: Physical, vol. 75, no. 3, pp. 242 – 251, 1999.

[2]. M. Daigle, J. Corcos, and K. Wu, "An analytical solution to circular touch mode capacitor," IEEE Sensors Journal, vol. 7, no. 4, pp. 502–505, 2007.

[3]. Y. Hezarjaribi, M. N. Hamidon, S. H. Keshmiri, and A. R. Bahadorimehr, "Capacitive pressure sensors based on MEMS operating in harsh environments," in ICSE 2008 Proceedings, Johor Bahru, Malaysia, 2008.

[4]. G. Meng and W. H. Ko, "Modeling of circular diaphragm and spreadsheet solution programming for touch mode capacitive sensors," Sensors and Actuators A: Physical, vol. 75, no. 1, pp. 45 – 52, 1999.

[5]. G. Fragiacomo, T. Ansbæk, T. Pedersen, O. Hansen, and E. V. Thomsen, "Analysis of small deflection touch mode behavior in capacitive pressure sensors," Sensors and Acutators A: Physical, vol. 161, pp. 114–119, 2010.

[6]. R. Wang, W. H. Ko, and D. J. Young, "Silicon-carbide-MESFET-based 4000C MEMS sensing and data telemetry," IEEE Sensors Journal, vol. 5, pp. 1389–1394, 2005.

[7]. W.-K. Chen, The VLSI Handbook, Second Edition (Electrical Engineering Handbook). Boca Raton, FL, USA: CRC Press, Inc., 2006.

[8]. S. D. Arthur, D. M. Brown, and K. S. Matocha, "Silicon carbide semiconductor structures, devices, and methods for making the same," 02 2011.

[9]. L. Chen, Silicon Carbide Pressure Sensors and Infra-Red Emitters. PhD. thesis, Case Western Reserve University, 2008.

[10]. S. P. Timoshenko and S. Woinowsky-Krieger, Theory of Plates and Sheels, Second Edition, McGraw- Hill, 1959.

Appendix

A more accurate expression for $\widehat{a_0}$ can be derived by taking α and σ_i into consideration and using (2) to substitute for a_v in (4). This procedure results in

$$a_0 \geq \widehat{a_0} = \sqrt{\frac{4t_d S(-\Lambda)}{\pi\varepsilon_0\varepsilon_d M^2}} \qquad (12)$$

and

$$P_T = \frac{\left(-\frac{M}{2\Lambda}\right)^2 + \sqrt{\left(-\frac{M}{2\Lambda}\right)^4 + 4}}{2} P_T' \qquad (13)$$

where

$$\Lambda = \frac{P_2 - P_2}{\Delta} . P_T'^2 [1 + 2(k_1 - k_2)(1-\gamma)] \left\{ \frac{P_2 - P_1}{P_T'} + \frac{2}{3}\left[\left(1 + \frac{P_2}{P_T'}\right)^{\frac{3}{2}} - \left(1 + \frac{P_1}{P_T'}\right)^{\frac{3}{2}} \right] \right\}$$

$$- \frac{P_2^2 - P_1^2}{\Delta} . P_T' [1 + 2(k_1 - k_2)(1-\gamma)] \left\{ \sqrt{\left(1 + \frac{P_2}{P_T'}\right)} - \sqrt{\left(1 + \frac{P_1}{P_T'}\right)} + \ln\left(\frac{\sqrt{1 + \frac{P_2}{P_T'}} - 1}{\sqrt{1 + \frac{P_1}{P_T'}} - 1} \right) \right\}$$

$$M = \frac{4(P_2 - P_1)}{\Delta} . P_T'^2 [k_2(1-\gamma) - 1] \left\{ \begin{array}{l} \frac{2}{7}\left[\left(\sqrt{1 + \frac{P_2}{P_T'}} - 1 \right)^{\frac{7}{2}} - \left(\sqrt{1 + \frac{P_1}{P_T'}} - 1 \right)^{\frac{7}{2}} \right] \\ + \frac{6}{5}\left[\left(\sqrt{1 + \frac{P_2}{P_T'}} - 1 \right)^{\frac{5}{2}} - \left(\sqrt{1 + \frac{P_1}{P_T'}} - 1 \right)^{\frac{5}{2}} \right] \\ + \frac{4}{3}\left[\left(\sqrt{1 + \frac{P_2}{P_T'}} - 1 \right)^{\frac{3}{2}} - \left(\sqrt{1 + \frac{P_1}{P_T'}} - 1 \right)^{\frac{3}{2}} \right] \end{array} \right\}$$

$$- \frac{2(P_2^2 - P_1^2)}{\Delta} . P_T' [k_2(1-\gamma) - 1] \left\{ \frac{2}{3}\left[\left(\sqrt{1 + \frac{P_2}{P_T'}} - 1 \right)^{\frac{3}{2}} - \left(\sqrt{1 + \frac{P_1}{P_T'}} - 1 \right)^{\frac{3}{2}} \right] + 2\left(\sqrt{\sqrt{1 + \frac{P_2}{P_T'}} - 1} - \sqrt{\sqrt{1 + \frac{P_1}{P_T'}} - 1} \right) \right\}$$

and

$$P_T' = \frac{\sigma_i^2 h^2 g}{16D\left[1 + 2\alpha\left(\frac{g}{h}\right)^2\right]}$$